

A phenomenological investigation of the beauty content of a
proton in the framework of k_t -factorization using KMR and MRW
unintegrated parton distributions

N. Olanj*

*Department of Physics, Faculty of Science,
Bu-Ali Sina University, 65178, Hamedan, Iran*

Abstract

In this paper, we address the reduced beauty cross section ($\sigma_{red}^{b\bar{b}}(x, Q^2)$) and the beauty structure function ($F_2^{b\bar{b}}(x, Q^2)$), to study the beauty content of a proton. We calculate $\sigma_{red}^{b\bar{b}}$ and $F_2^{b\bar{b}}$ in the k_t -factorization formalism by using the integral form of the *Kimber-Martin-Ryskin* and *Martin-Ryskin-Watt* unintegrated parton distribution function (*KMR* and *MRW-UPDF*) with the angular ordering constraint (*AOC*) and the *MMHT2014 PDF* set as the input. Recently Guiot and van Hameren demonstrated that the upper limit, k_{max} , of the transverse-momentum integration performed in the k_t -factorization formalism should be almost equal to Q , where Q is the hard scale, otherwise it leads to an overestimation of the proton structure function ($F_2(x, Q^2)$). In the present work, we show that k_{max} cannot be equal to Q at low and moderate energy region, and also by considering the gluon and quark contributions to the same perturbative order and a physical gauge for the gluon, i.e., $A^\mu q'_\mu = 0$ in the calculation of $F_2^{b\bar{b}}$ in the k_t -factorization formalism, we do not encounter any overestimation of the theoretical predictions due to different choices of $k_{max} > Q$. Finally, the resulted $\sigma_{red}^{b\bar{b}}$ and $F_2^{b\bar{b}}$ are compared to the experimental data and the theoretical predictions. In general, the extracted $\sigma_{red}^{b\bar{b}}$ and $F_2^{b\bar{b}}$ based on the *KMR* and *MRW* approaches are in perfect agreement with the experimental data and theoretical predictions at high energies, but at low and moderate energies, the one developed from the *KMR* approach has better consistency than that of *MRW* approach.

PACS numbers: 12.38.Bx, 13.85.Qk, 13.60.-r

Keywords: k_t -factorization, *unintegrated* parton distribution function, *DGLAP* equation, reduced beauty cross section, beauty structure function

*Corresponding author, Email: *n_olanj@basu.ac.ir*, Tel: +98-81-31400000

I. INTRODUCTION

The study of the charm and beauty content of a proton in deep inelastic ep scattering at *HERA* plays an important role in the investigation of the theory of the perturbative quantum *chromodynamics* ($pQCD$) at the small *Bjorken* scale (x) [1–3], the electroweak Higgs boson production at the *LHC* [4] and hadron-hadron differential cross sections.

Recently, we investigated the charm content of a proton in the frameworks of the *KMR* [5] and *MRW* [6] approaches by calculating the charm structure function $F_2^{c\bar{c}}(x, Q^2)$ [7] in the k_t -factorization formalism [8–12]. We showed that the calculated charm structure functions by using the *MRW-UPDF* and *KMR-UPDF* are consistent with the experimental data and the theoretical predictions based on the general-mass variable-flavor-number scheme (*GMVFNS*) [13], the *LO* collinear procedure and the saturation model introduced by *Golec – Biernat* and *Wüsthoff* (*GBW*) [14]. Also, in the reference [15], the b -quark contribution to the inclusive proton structure function $F_2(x, Q^2)$ at high values of Q^2 has been investigated at the leading-order k_t -factorization approach using *KMR-UPDF* and only considering the gluon contribution.

Recently, in the reference [16], measurements of charm and beauty production cross section in deep inelastic ep scattering at *HERA* from the *H1* and *ZEUS* Collaborations are combined and results for the so-called reduced charm and beauty cross section ($\sigma_{red}^{q\bar{q}}(x, Q^2), q = c, b$) are obtained in the kinematic range of negative four-momentum transfer squared ($-q^2 = Q^2$) of the photon $2.5 GeV^2 \leq Q^2 \leq 2000 GeV^2$ and Bjorken scaling variable $3 \times 10^{-5} \leq x_{Bj} \leq 5 \times 10^{-2}$. The double-differential cross section for the production of a heavy flavour of type q ($q = c, b$) may then be written in terms of the heavy-flavour contributions of the structure functions $F_2(x, Q^2)$ ($F_T(x, Q^2) + F_L(x, Q^2)$) and $F_L(x, Q^2)$ [17, 18], as follows:

$$\begin{aligned} \frac{d^2\sigma^{q\bar{q}}}{dx dQ^2} &= \frac{4\pi\alpha^2(Q^2)}{Q^4} \left[\frac{1 + (1-y)^2}{2x} F_T^{q\bar{q}}(x, Q^2) + \frac{1-y}{x} F_L^{q\bar{q}}(x, Q^2) \right] \\ &= \frac{2\pi\alpha^2(Q^2)}{xQ^4} \left[(1 + (1-y)^2) F_2^{q\bar{q}}(x, Q^2) - y^2 F_L^{q\bar{q}}(x, Q^2) \right], \end{aligned} \quad (1)$$

where $y = \frac{Q^2}{xs}$ (s is *CM* energy squared) denotes the lepton inelasticity, the fraction of energy transferred from the electron in the fixed proton frame. The reduced cross sections

are defined, as follows:

$$\begin{aligned}\sigma_{red}^{q\bar{q}}(x, Q^2) &= \frac{d^2\sigma^{q\bar{q}}}{dx dQ^2} \cdot \frac{xQ^4}{2\pi\alpha^2(Q^2)(1+(1-y)^2)} \\ &= F_2^{q\bar{q}}(x, Q^2) - \frac{y^2}{1+(1-y)^2} F_L^{q\bar{q}}(x, Q^2).\end{aligned}\quad (2)$$

In expressing the importance of the investigation of the proton beauty contents in this paper, it should be noted that the reduced cross section ($\sigma_{red}^{q\bar{q}}(x, Q^2)$) is dependent on the heavy-flavour longitudinal structure function ($F_L^{q\bar{q}}(x, Q^2)$). Therefore, since the longitudinal structure function is directly sensitive to the gluon distributions, the calculations of the reduced cross section are beyond the standard collinear factorization procedure i.e. the k_t -factorization formalism.

In this work, we use the integral form of *MRW-UPDF* and *KMR-UPDF* with the angular ordering constraint (*AOC*) [19] and the ordinary parton distribution functions (the cutoff independent *PDF*) according to the investigations carried out in the references [19] and [20] as input in the k_t -factorization formalism to calculate the reduced cross section of production of a beauty quark pair in the final state of the deep inelastic ep scattering, ($\sigma_{red}^{b\bar{b}}(x, Q^2)$) and the beauty structure function ($F_2^{b\bar{b}}(x, Q^2)$). It is worth mentioning that in the references [19] and [20], it is stated that " the differential version of *KMR* prescription and the implementations of angular (strong) ordering constraints (*AOC* (*SOC*)), cause the negative-discontinuous *UPDF* with the ordinary parton distribution functions as the input and finally leads to results far from experimental data, but those the proton (longitudinal) structure functions calculated based on the integral prescription of the *KMR-UPDF* with the *AOC* and the ordinary *PDF* as the input are reasonably consistent with the experimental data." Then the predictions of these two approaches by using the *MMHT2014-LO* and *MMHT2014-NLO* set of the *PDF* [21] as input for the reduced beauty cross section are compared to the combined data of the *H1* and *ZEUS* Collaborations at *HERA* [16] and theoretical predictions based on the *HERAPDF2.0 FF3A* set [22]. Also, the resulted beauty structure function is compared to the predictions of the *MSTW08 – NLO QCD* fits [23] and the *ZEUS* measurements [24–26]. As shown in references [27, 28], *UPDF* with different input *PDF* sets are almost very similar and stable, so we can still use *MMHT2014 PDF* set instead of the new *MSHT20 PDF* set [29] in this work. In general, it is shown that the calculated reduced beauty cross section ($\sigma_{red}^{b\bar{b}}$) and the beauty structure function ($F_2^{b\bar{b}}$) based on the *UPDF* of the two approaches are very consistent with the experimental

data, especially at high energies. However, the reduced beauty cross sections and the beauty structure functions, which are extracted from the *KMR* approach, have a better agreement with the experimental data with respect to that of *MRW* at low and moderate energies.

It should be noted that the k_t -factorization formalism is computationally more straightforward than the theory of the $pQCD$. The discrepancy between the $pQCD$ and the k_t -factorization prediction can be reduced by refitting the input integrated *PDF* [30] and using the cut-off dependent *PDF* [31]. As explained in the reference [30], this treatment is adequate for initial investigations and descriptions of exclusive processes.

It is worth mentioning that recently Guiot and van Hameren (*GvH*) encountered an overestimation of the exact structure function by calculate the proton structure function ($F_2(x, Q^2)$) in the k_t -factorization formalism at order $O(\lambda^2)$, with λ the coupling of the Yukawa theory by using the differential form of the *KMRW* – *UPDF* computed in the Yukawa theory only considering the quark contributions [32]. Therefore, *GvH* argued that the upper limit, k_{max} , of the transverse-momentum integration performed in the k_t -factorization formalism is equal to $\mu_F \sim Q$ (Q is the hard scale) used to factorize the cross section into an off-shell hard coefficient and a universal factor. In the present work, we show that k_{max} cannot be equal to Q at low and moderate energy region ($2.5 GeV^2 \leq Q^2 \leq 120 GeV^2$), and also by considering the gluon and quark contributions to the same perturbative order and a physical gauge for the gluon, i.e., $A^\mu q'_\mu = 0$ in the calculation of $F_2^{b\bar{b}}(x, Q^2)$ and $F_L^{b\bar{b}}(x, Q^2)$ in the k_t -factorization formalism, we do not encounter any overestimation of the theoretical predictions due to different choices of $k_{max} > Q$.

Due to the importance of this subject, in our previous articles, we investigated the general behavior and stability of the *KMR* and *MRW* approaches [27, 33–40] and in this paper, we study the beauty content of a proton by examining the reduced cross section ($\sigma_{red}^{b\bar{b}}(x, Q^2)$) and the beauty structure function ($F^{b\bar{b}}(x, Q^2)$). Also, we have successfully used *KMR-UPDF* in our previous articles, to calculate the inclusive production of the W and Z gauge vector bosons [41, 42], the semi-*NLO* production of *Higgs* bosons [43], the production of forward-center and forward-forward di-jets [44], the prompt-photon pair production [45], the single-photon production [46] and the charm structure function[7]. We explored the phenomenology of the integral and the differential versions of the *KMR-UPDF* using the angular (strong) ordering (*AOC* (*SOC'*)) constraints in the reference [19]. Also, among the applications of these *UPDF*, one can refer to the references [47–50].

So, the paper is organized as follows: an overview of the *KMR* and *MRW* approaches to generating *UPDF* and calculation of the beauty contribution to the proton structure function ($F_2^{b\bar{b}}(x, Q^2)$) and the proton longitudinal structure function ($F_L^{b\bar{b}}(x, Q^2)$) based on the k_t -factorization formalism are provided in section *II*. Finally, the results of the reduced beauty cross section and the beauty structure function in the k_t -factorization formalism using the *KMR-UPDF* and *MRW-UPDF* as input are presented in section *III*.

II. *KMR-UPDF*, *MRW-UPDF* APPROACHES AND $F_2^{b\bar{b}}(x, Q^2)$ AND $F_L^{b\bar{b}}(x, Q^2)$ IN THE k_t -FACTORIZATION FORMALISM

A brief review of the *KMR* [5] and *MRW* [6] approaches to generating *UPDF* ($f_a(x, k_t^2, \mu^2)$ at the *LO* and *NLO* levels, respectively, where x , k_t , and μ are the longitudinal momentum fraction, the transverse momentum, and the factorization scale, respectively) is provided in this section. The *KMR* and *MRW* formalisms are based on the *DGLAP* equations using some modifications due to the separation of the virtual and real parts of the evolutions.

The *KMR* approach leads to the following integral forms for the quark and gluon *UPDF* at the *LO* level, respectively:

$$\begin{aligned} f_q(x, k_t^2, \mu^2) &= T_q(k_t, \mu) \frac{\alpha_s(k_t^2)}{2\pi} \\ &\times \int_x^{1-\Delta} dz \left[P_{qq}(z) \frac{x}{z} q\left(\frac{x}{z}, k_t^2\right) \right. \\ &\quad \left. + P_{qg}(z) \frac{x}{z} g\left(\frac{x}{z}, k_t^2\right) \right], \end{aligned} \quad (3)$$

$$\begin{aligned} f_g(x, k_t^2, \mu^2) &= T_g(k_t, \mu) \frac{\alpha_s(k_t^2)}{2\pi} \\ &\times \int_x^{1-\Delta} dz \left[\sum_q P_{gq}(z) \frac{x}{z} q\left(\frac{x}{z}, k_t^2\right) \right. \\ &\quad \left. + P_{gg}(z) \frac{x}{z} g\left(\frac{x}{z}, k_t^2\right) \right], \end{aligned} \quad (4)$$

where $P_{aa'}(x)$ are the corresponding splitting functions and the survival probability factors,

T_a , is evaluated from:

$$T_a(k_t, \mu) = \exp \left[- \int_{k_t^2}^{\mu^2} \frac{\alpha_s(k_t'^2)}{2\pi} \frac{dk_t'^2}{k_t'^2} \right] \times \sum_{a'} \int_0^{1-\Delta} dz' P_{a'a}(z'), \quad (5)$$

where Δ is a cutoff to prevent the integrals from becoming singular at $z = 1$ (arises from the soft gluon emission). By considering the angular ordering constraint (*AOC*), which is the consequence of the coherent gluon emissions, the cutoff is equal to $\frac{k_t}{\mu+k_t}$ and *UPDF* extend smoothly into the domain $k_t > \mu$. It should be mentioned that in this approach, T_a is considered to be unity for $k_t > \mu$. Therefore $k_{max} = \mu \sim Q$ is not an intrinsic property of the the unintegrated parton distribution function.

The *MRW* approach leads to the following integral forms for the quark and gluon *UPDF* at the *NLO* level:

$$f_a(x, k_t^2, \mu^2) = \int_x^1 dz T_a(k^2, \mu^2) \frac{\alpha_s(k^2)}{2\pi} \times \sum_{b=q,g} P_{ab}^{(0+1)}(z) b\left(\frac{x}{z}, k^2\right) \Theta(\mu^2 - k^2), \quad (6)$$

where

$$P_{ab}^{(0+1)}(z) = P_{ab}^{(0)}(z) + \frac{\alpha_s}{2\pi} P_{ab}^{(1)}(z),$$

$$k^2 = \frac{k_t^2}{1-z}, \quad (7)$$

and

$$T_a(k^2, \mu^2) = \exp \left(- \int_{k^2}^{\mu^2} \frac{\alpha_s(\kappa^2)}{2\pi} \frac{d\kappa^2}{\kappa^2} \right) \times \sum_{b=q,g} \int_0^1 d\zeta \zeta P_{ba}^{(0+1)}(\zeta). \quad (8)$$

$P_{ab}^{(0)}$ and $P_{ab}^{(1)}$ functions in the above equations correspond to the *LO* and *NLO* contributions of the splitting functions, respectively, which are given in the reference [51]. In the *MRW* approach, unlike the *KMR* approach, the cutoff is imposed only on the terms in which the splitting functions are singular, i.e., the terms that include P_{qq} and P_{gg} , also, the scale $k^2 = \frac{k_t^2}{1-z}$ is used instead of the scale k_t^2 . For more details see reference [36].

In the following, we briefly present the formulations of the beauty structure function ($F_2^{b\bar{b}}(x, Q^2)$) and the beauty longitudinal structure function ($F_L^{b\bar{b}}(x, Q^2)$) in the k_t -factorization formalism. By considering the gluon and quark contributions to the same perturbative order and a physical gauge for the gluon, i.e., $A^\mu q'_\mu = 0$ ($q' = q + xp$), the beauty structure function $F_2^{b\bar{b}}(x, Q^2)$ is given by the sum of the gluon contribution (the subprocess $g \rightarrow q\bar{q}$, the equation (9)) and the quark contribution (the subprocess $q \rightarrow qg$, the equation (13)) according to the equations (8) and (12) of the reference [7].

For the gluon contribution:

$$F_{2g \rightarrow q\bar{q}}^{b\bar{b}}(x, Q^2) = e_b^2 \frac{Q^2}{4\pi} \int_{k_0^2}^{k_{max}^2} \frac{dk_t^2}{k_t^4} \int_0^1 d\beta \int_{k_0^2}^{k_{max}^2} d^2\kappa_t \alpha_s(\mu^2) f_g\left(\frac{x}{z}, k_t^2, \mu^2\right) \Theta(1 - \frac{x}{z}) \left\{ [\beta^2 + (1 - \beta^2)] \left(\frac{\kappa_{\mathbf{t}}}{D_1} - \frac{(\kappa_{\mathbf{t}} - \mathbf{k}_{\mathbf{t}})}{D_2} \right)^2 + [m_b^2 + 4Q^2\beta^2(1 - \beta)^2] \left(\frac{1}{D_1} - \frac{1}{D_2} \right)^2 \right\}, \quad (9)$$

where

$$\begin{aligned} D_1 &= \kappa_t^2 + \beta(1 - \beta)Q^2 + m_b^2, \\ D_2 &= (\kappa_{\mathbf{t}} - \mathbf{k}_{\mathbf{t}})^2 + \beta(1 - \beta)Q^2 + m_b^2, \end{aligned} \quad (10)$$

and

$$\frac{1}{z} = 1 + \frac{\kappa_t^2 + m_b^2}{(1 - \beta)Q^2} + \frac{k_t^2 + \kappa_t^2 - 2\kappa_{\mathbf{t}} \cdot \mathbf{k}_{\mathbf{t}} + m_b^2}{\beta Q^2}, \quad (11)$$

where in the above equations, the variable β is defined as the light-cone fraction of the photon momentum carried by the internal quark and k_0 is chosen to be about 1 GeV. The graphical representations of k_t and κ_t are introduced in the figure 7 of the reference [36]. The scale μ controls both the unintegrated partons and the QCD coupling constant (α_s) and it is chosen as follows:

$$\mu^2 = k_t^2 + \kappa_t^2 + m_b^2. \quad (12)$$

It should be mentioned that the imposition of angular ordering constraint (AOC) at the last step of the evolution instead of the strong ordering constraint (SOC) leads to physically reasonable unintegrated parton distribution functions which extend smoothly into the domain $k_t > \mu$ [5]. Therefore, the acceptable value of k_{max} is the value that does not change the result of structure function by increasing it. For example, in the reference [17], k_{max} is considered equal to $4Q$.

For the quark contribution:

$$F_{2q \rightarrow qg}^{b\bar{b}}(x, Q^2) = e_b^2 \int_{k_0^2}^{Q^2} \frac{d\kappa_t^2}{\kappa_t^2} \frac{\alpha_s(\kappa_t^2)}{2\pi} \int_{k_0^2}^{\kappa_t^2} \frac{dk_t^2}{k_t^2} \int_x^{\frac{Q}{(Q+k_t)}} dz \left[f_b\left(\frac{x}{z}, k_t^2, Q^2\right) + f_{\bar{b}}\left(\frac{x}{z}, k_t^2, Q^2\right) \right] P_{qq}(z). \quad (13)$$

In this paper, the mass of beauty quark is considered to be $m_b = 4.18 \text{ GeV}$. See reference [7] for more details.

As mentioned in reference [7], the dominant mechanism of the proton c, b -quark electro-production is the subprocess $g \rightarrow qq$, and since we are working in the small x region (i.e. the high energy region), we ignored the contribution of the non-perturbative region. According to the above, the beauty longitudinal structure function ($F_L^{b\bar{b}}(x, Q^2)$) in the k_t -factorization approach is presented as follows:

$$F_L^{b\bar{b}}(x, Q^2) = \frac{Q^4}{\pi^2} e_b^2 \int_{k_0^2}^{k_{max}^2} \frac{dk_t^2}{k_t^4} \Theta(k^2 - k_0^2) \int_0^1 d\beta \int_{k_0^2}^{k_{max}^2} d^2\kappa_t \alpha_s(\mu^2) \beta^2 (1 - \beta)^2 \left(\frac{1}{D_1} - \frac{1}{D_2} \right)^2 \times f_g\left(\frac{x}{z}, k_t^2, \mu^2\right) + e_b^2 \frac{\alpha_s(Q^2)}{\pi} \frac{4}{3} \int_x^1 \frac{dy}{y} \left(\frac{x}{y}\right)^2 [q(y, Q^2) + \bar{q}(y, Q^2)], \quad (14)$$

where $y = x \left(1 + \frac{\kappa_t'^2 + m_b^2}{\beta(1-\beta)Q^2} \right)$ (in which $\kappa_t' = \kappa_t - (1 - \beta)\mathbf{k}_t$) and the variables of the above equation are the same as the variables of the beauty structure function ($F_2^{b\bar{b}}(x, Q^2)$). It should be noted that the first term is derived with the use of a pure gluon contribution from the perturbative region in the k_t -factorization approach. The second term is the beauty quark contribution in the longitudinal structure function which comes from the collinear factorization.

III. RESULTS, DISCUSSIONS AND CONCLUSIONS

As mentioned before, the purpose of this work is a detailed investigation of the beauty content of a proton in the framework of k_t -factorization using KMR and MRW approaches to generate the $UPDF$, validate these two approaches and also investigation the upper limit of transverse momentum (k_{max}) in the k_t -factorization formalism. For this purpose, the reduced beauty cross sections ($\sigma_{red}^{b\bar{b}}(x, Q^2)$, the equation (2)) are calculated by using the beauty structure functions ($F_2^{b\bar{b}}(x, Q^2)$, the sum of the equations (9) and (13)) and the beauty longitudinal structure functions ($F_L^{b\bar{b}}(x, Q^2)$, the equation (14)) in the k_t -factorization

formalism. The integral form of $KMR-UPDF$ and $MRW-UPDF$, i.e., the equations (3), (4) and (6) with the angular ordering constraint (AOC) are used as input of the beauty structure functions and the beauty longitudinal structure functions in the k_t -factorization formalism with different $k_{max} \geq Q$.

In the figures 1, the reduced beauty cross section ($\sigma_{red}^{b\bar{b}}$) are displayed in the framework of k_t -factorization using the KMR and MRW approaches as a function of x for different values of $Q^2 = 2.5, 5, 7, 12, 18, 32, 60, 120, 200, 350, 650$ and 2000 GeV^2 with the input $MMHT2014$ set of PDF (to generate the $UPDF$) at the LO and NLO approximations, respectively, with $k_{max}^2 = Q^2, 16Q^2$ in all panels, $k_{max}^2 = 36Q^2$ in panels a, b and c and $k_{max}^2 = 10^4 \text{ GeV}^2$ in panels c and i. These results are compared to the combined data of the $H1$ and $ZEUS$ Collaborations at $HERA$ [16] (the full circle points) and theoretical predictions based on the $HERAPDF2.0 \text{ FF3A}$ set [22] (dash-dot curves). In the figure 2, the obtained results from the calculations of the beauty structure functions are presented as a function of Q^2 for various x values using the KMR ($MMHT2014 - LO \text{ PDF}$, dash curves) and MRW ($MMHT2014 - NLO \text{ PDF}$, full curves) approaches with $k_{max}^2 = Q^2$ (at $i = 0, 2$ and 7), $16Q^2$ (at all i) and 10^4 GeV^2 (at $i = 2$ and 7). These results are compared to the experimental measurements of $ZEUS$ (filled circles [2], open circles [25] and open triangles [26]) and the predictions of $MSTW08 - NLO \text{ QCD}$ calculations [23]. To provide a clear comparison between the frameworks of the KMR and MRW approaches, we have plotted the $KMR - UPDF$ (dash curves) and $MRW - UPDF$ (full curves) versus k_t^2 at typical values of $x = 0.01, 0.001$ and 0.0001 and the factorization scales $Q^2 = 60$ and 350 GeV^2 for the beauty and gluon partons, in the figure 3. Also, the beauty and gluon PDF at scales $Q^2 = 60$ and 350 GeV^2 are plotted by using the $MMHT2014-LO$ (dash curves) and $MMHT2014-NLO$ (full curves) [21] in figure 4. It should be mentioned that in the calculations related to the figures 1, 2 and 3, we consider the QCD coupling constant, $\alpha_s(M_z^2)$, to be the same as those used in fitting the input PDF to the $KMR - UPDF$ and $MRW - UPDF$, i.e. $\alpha_{s,LO}(M_z^2) = 0.135$ and $\alpha_{s,NLO}(M_z^2) = 0.118$, respectively.

In general, the extracted $\sigma_{red}^{q\bar{q}}$ and $F_2^{b\bar{b}}(x, Q^2)$ based on both the KMR and MRW approaches are in perfect consistent with the experimental data [16, 23] and the theoretical predictions [2, 22, 25, 26] at high energies, but the one developed from the KMR approach has a better agreement with the experimental data and the theoretical predictions with respect to that of MRW approach at low and moderate energies.

As shown in the figures 1 and 2, and we expected according to the figures 3 and 4 (see panels d and j of the figure 3 (the large x and high energy region) and the figure 4), the results of the KMR and MRW approaches are very close to each other at the high hard scale (Q^2) and large x , but they become separated as the hard scale and x decrease. It should be noted that this decrease in difference with increasing hard scale Q and x is due to the use of the scale $k^2 = \frac{k_t^2}{1-z}$, the coupling constant $\alpha_{s,NLO}(M_z^2) = 0.118$ and $MMHT2014-NLO$ PDF set instead of the scale k_t^2 , the coupling constant $\alpha_{s,LO}(M_z^2) = 0.135$ and $MMHT2014-LO$ PDF set in the MRW approach. Note that this decrease cannot be a result of different use of cut-off and splitting functions.

It is clear in the figures 1 and 2 that at low and moderate x and low energy region (see the first 8 panels of the figure 1, $Q^2 \leq 120 GeV^2$ and $i = 7$ in the figure 2), there is no good agreement between the experimental data and the obtained results considering $k_{max}^2 = Q^2$ and this is due to the non-negligibility value of $KMR-UPDF$ in the $k_t > Q$ region at low x and Q^2 (see panels c and i of the figure 3). But the results obtained from both KMR and MRW approaches, considering $K_{max}^2 \geq 16Q^2$, have a good agreement with the theoretical predictions in all panels of the figures 1 and 2 (as mentioned in reference [17]). Also, at large x and high energy region (see the last 4 panels of the figure 1, $Q^2 \geq 200 GeV^2$ and $i = 2$ in the figure 2), with the increase of k_{max}^2 from Q^2 to 10^4 , the results are almost the same and this is due to the negligible value of $KMR-UPDF$ and $MRW-UPDF$ in the $k_t > Q$ region at large x and high values of Q^2 (see panels d and j of the figure 3). It should be noted that according to the figures 1 and 2, we do not encounter any overestimation of the theoretical predictions with increasing k_{max} .

Also, as it is clear in the figures 1 and 2, at high (low) energy region, the result of the reduced beauty cross section and the beauty structure functions calculations have not changed by increasing k_{max} from Q to $10Q$ (from $4Q$ to $10Q$), so $k_{max}=Q$ ($k_{max}=4Q$) can be considered to save calculation time at high (low) energy.

It should be mentioned that the k_t -factorization is more computationally simpler than $pQCD$ and is adequate for initial investigations and descriptions of exclusive processes [30]. The results of this paper are another confirmation of this matter. As it has been explained in the reference [30], we expect to reduce the discrepancy between the data and the k_t -factorization prediction by refitting the input integrated PDF and using the cut-off dependent PDF [31] as the input for the $UPDF$.

In conclusion, the extracted $\sigma_{red}^{b\bar{b}}(x, Q^2)$ and $F_2^{b\bar{b}}(x, Q^2)$ in the k_t -factorization formalism by using the $KMR - UPDF$ and $MRW - UPDF$ are in a good agreement with the predictions of the $pQCD$ and the experimental data, but those that are extracted from the KMR approach, have a perfect agreement with the experimental data. This issue cannot be unrelated to the consideration of $T_a = 1$ for $k_t > \mu$, which leads to the contribution of a NLO effect in the calculation of $KMR-UPDF$ [5]. Also, according to the study conducted on the upper limit, k_{max} , of the transverse-momentum integration performed in the k_t -factorization formalism, we hope that the computation time of the cross section at high energy region will be reduced by considering $k_{max} = Q$.

Acknowledgments

I would like to acknowledge the University of Bu-Ali Sina for their support.

-
- [1] G. Pancheri and Y. N. Srivastava, Eur. Phys. J. C **17** (2017) 150.
 - [2] ZEUS collaboration, H. Abramowicz et al., JHEP **09** (2014) 127.
 - [3] R. Gauld, U. Haisch, B. D. Pecjak, and E. Re, Phys. Rev. D **92** (2015) 034007.
 - [4] F. Maltoni, Z. Sullivan, and S. Willenbrock, Phys. Rev. D **67** (2003) 093005.
 - [5] M. A. Kimber, A. D. Martin, and M. G. Ryskin, Phys. Rev. D **63** (2001) 114027.
 - [6] A. D. Martin, M. G. Ryskin, and G. Watt, Eur. Phys. J. C **66** (2010) 163.
 - [7] N. Olanj and M. Modarres, Nucl. Phys. A **998** (2020) 121735.
 - [8] S. Catani, M. Ciafaloni and F. Hautmann, Phys. Lett. B **242** (1990) 97.
 - [9] S. Catani, M. Ciafaloni and F. Hautmann, Nucl. Phys. B **366** (1991) 657.
 - [10] J.C. Collins and R.K. Ellis, Nucl. Phys. B **360** (1991) 3.
 - [11] S. Catani and F. Hautmann, Nucl. Phys. B **427** (1994) 475.
 - [12] M. Ciafaloni, Phys. Lett. **356** (1995) 74.
 - [13] HERA Combined Results, *HERAPDF* table,
<https://www.desy.de/h1zeus/combined.results/herapdf/table>.
 - [14] L. Motyka and N. Timneanu, Eur. Phys. J. C **27** (2003) 73.
 - [15] A. V. Lipatov, N. P. Zotov, JHEP **08** (2006) 043.

- [16] H1 and ZEUS Collaborations, H. Abramowicz et al., Eur. Phys. J. C **78** (2018) 473.
- [17] M. A. Kimber, Unintegrated Parton Distributions (Ph.D. thesis), University of Durham, 2001.
- [18] R. K. Ellis, W. J. Stirling and B. R. Webber, QCD and Collider Physics, Cambridge University Press (1996).
- [19] N. Olanj and M. Modarres, Eur. Phys. J. C **79** (2019) 615.
- [20] K. Golec-Biernat, A.M. Stasto, Phys. Lett. B **781** (2018) 633.
- [21] L. A. Harland-Lang, A. D. Martin, P. Motylinski, R. S. Thorne, Eur. Phys. J. C **75** (2015) 204.
- [22] H. Abramowicz et al. [H1 and ZEUS Collaborations], Eur. Phys. J. C **75** (2015) 580.
- [23] A.D. Martin, W.J. Stirling, R.S. Thorne and G. Watt, Eur. Phys. J. C **63** (2009) 189.
- [24] ZEUS collaboration, H. Abramowicz et al., JHEP **09** (2014) 127.
- [25] ZEUS collaboration, S. Chekanov et al., Eur. Phys. J. C **65** (2010) 65.
- [26] ZEUS collaboration, H. Abramowicz et al., Eur. Phys. J. C **69** (2010) 347.
- [27] M. Modarres and H. Hosseinkhani, Few-Body Syst., **47** (2010) 237.
- [28] Z. Badieian Baghsiyahi, M. Modarresa, R. Kord Valeshabadi, Eur. Phys. J. C **82** (2022) 392.
- [29] S. Bailey, T. Cridge, L. A. Harland-Lang, A. D. Martin, R. S. Thorne, Eur. Phys. J. C **81** (2021) 341.
- [30] G. Watt, A. D. Martin and M. G. Ryskin, Phys. Rev. D, **70** (2004) 014012.
- [31] N. Olanj, M. Lotfi Parsa, L. Asgari, Physics Letters B **834** (2022) 137472.
- [32] B. Guiot and A. van Hameren, JHEP **04** (2024) 085.
- [33] H. Hosseinkhani, M. Modarres, N. Olanj, IJMPA **32** (2017) 1750121.
- [34] M. Modarres, M. R. Masouminia, H. Hosseinkhani, N. Olanj, Nucl. Phys. A **945** (2016) 168.
- [35] M. Modarres, H. Hosseinkhani, N. Olanj, M.R. Masouminia, Eur. Phys. J. C **75** (2015) 556.
- [36] M. Modarres, H. Hosseinkhani, and N. Olanj, Phys. Rev. D **89** (2014) 034015.
- [37] M. Modarres, H. Hosseinkhani, and N. Olanj, Nucl. Phys. A **902** (2013) 21.
- [38] M. Modarres and H. Hosseinkhani, Nucl. Phys. A **815** (2009) 40.
- [39] H. Hosseinkhani and M. Modarres, Phys. Lett. B **694** (2011) 355.
- [40] H. Hosseinkhani and M. Modarres, Phys. Lett. B **708** (2012) 75.
- [41] M. Modarres, M. R. Masouminia, R. Aminzadeh-Nik, H. Hoseinkhani, N. Olanj, Phys. Rev. D **94** (2016) 074035.
- [42] M. Modarres, M. R. Masouminia, R. Aminzadeh-Nik, H. Hoseinkhani, N. Olanj, Phys. Lett.

- B **772** (2017) 534.
- [43] M. Modarres, M. R. Masouminia, R. Aminzadeh-Nik, H. Hoseinkhani, N. Olanj, Nucl. Phys. B **926** (2018) 406.
- [44] M. Modarres, M. R. Masouminia, R. Aminzadeh-Nik, H. Hoseinkhani, N. Olanj, Nucl. Phys. B **922** (2017) 94.
- [45] M. Modarres, R. Aminzadeh-Nik, R. Kord Valeshbadi, H. Hosseinkhani and N. Olanj, J. Phys. G **46** (2019) 105005.
- [46] R. Aminzadeh Nik, M. Modarres, N. Olanj and R. Taghavi, Phys. Rev. D **103** (2021) 074020.
- [47] R. K. Valeshabadi, M. Modarres, S. Rezaie, and R. Aminzadeh-Nik, J. Phys. G **48** (2021) 085009.
- [48] R. K. Valeshabadi, M. Modarres, S. Rezaie, Phys. Rev. D **104** (2021) 054019.
- [49] R. K. Valeshabadi, M. Modarres, S. Rezaie, Eur. Phys. J. C **81** (2021) 961.
- [50] S. Rezaie, M. Modarres, Eur. Phys. J. C **83** (2023) 678.
- [51] W. Furmanski, R. Petronzio, Phys. Lett. B **97** (1980) 437.
- [52] I. Hinchliffe, A. Manohar, Ann. Rev. Nucl. Part. Sci. **50** (2000) 643.
- [53] G. Pancheri, Y. N. Srivastava, Eur. Phys. J. C **77** (2017) 150.

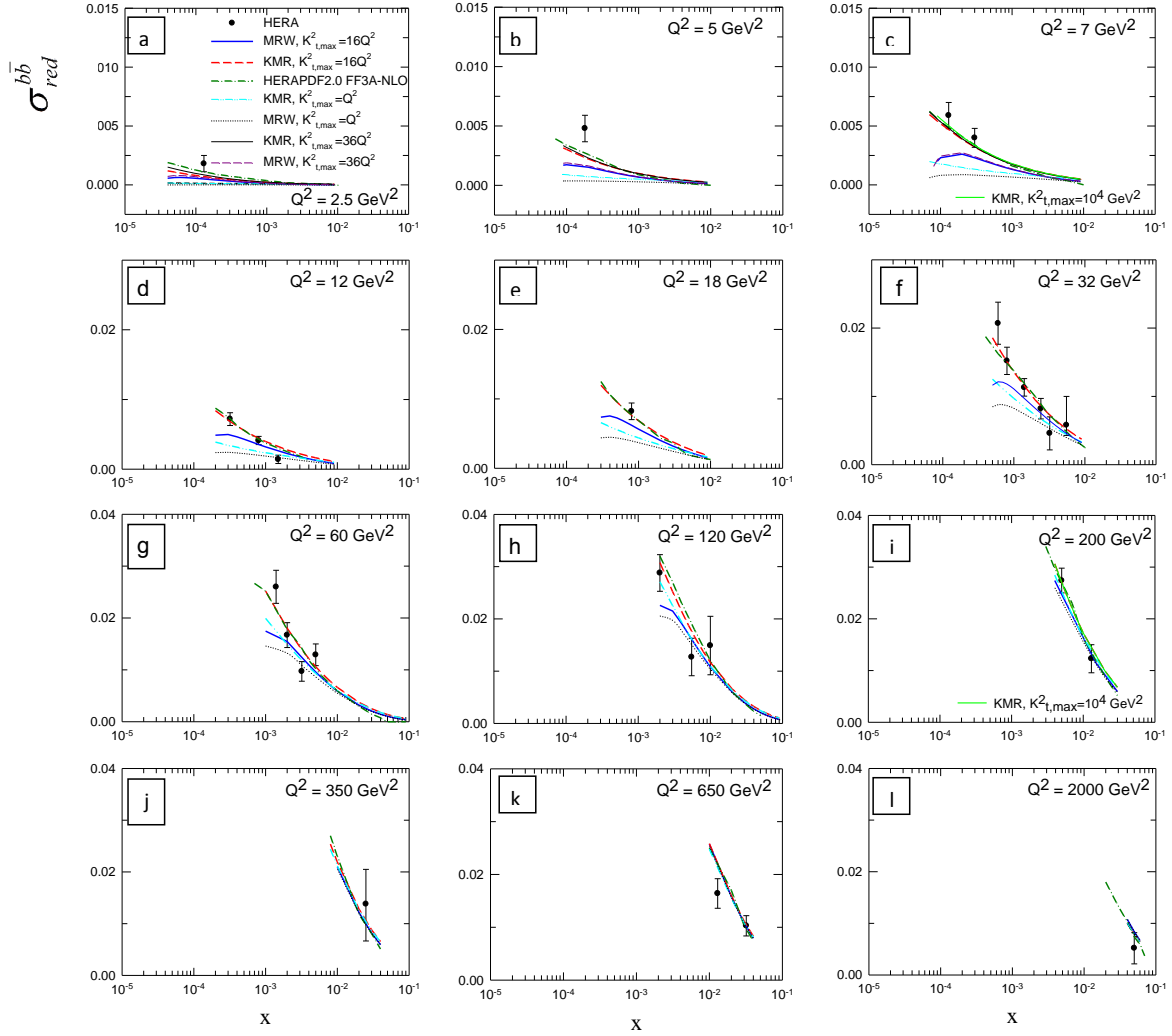


FIG. 1: The reduced beauty cross section as a function of x for various Q^2 values. See the text for more explanations.

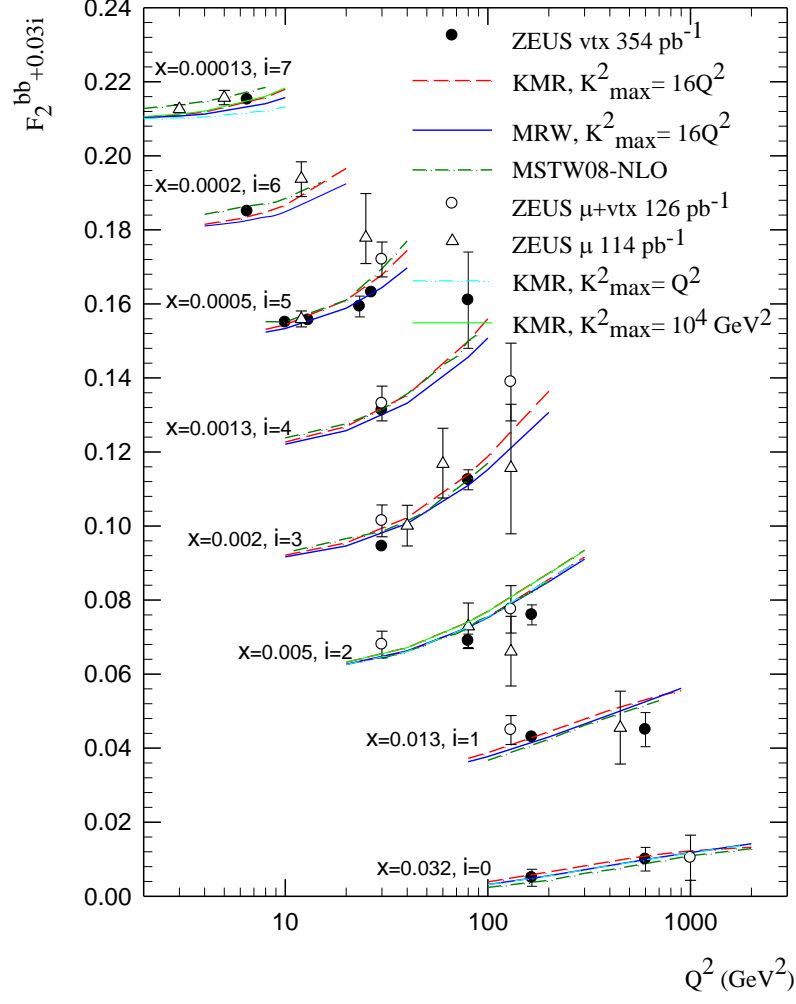


FIG. 2: The beauty structure function as a function of Q^2 for various x values. See the text for more explanations.

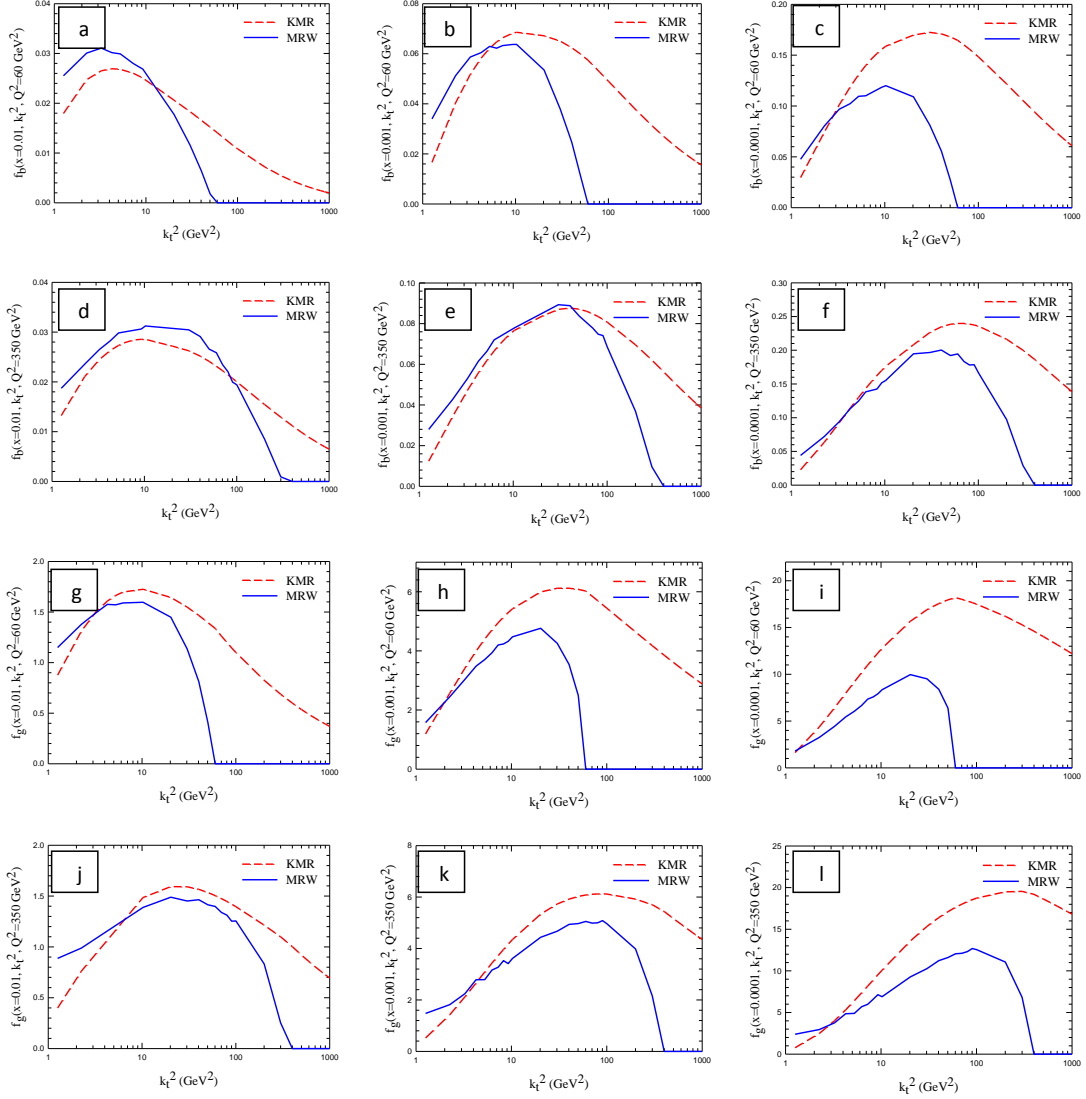


FIG. 3: The unintegrated beauty quark and gluon distribution functions versus k_t^2 with the *KMR* (*MRW*) prescription by using the *MMHT2014 $\overline{\text{NLO}}$* (*MMHT2014-NLO*) as the inputs.

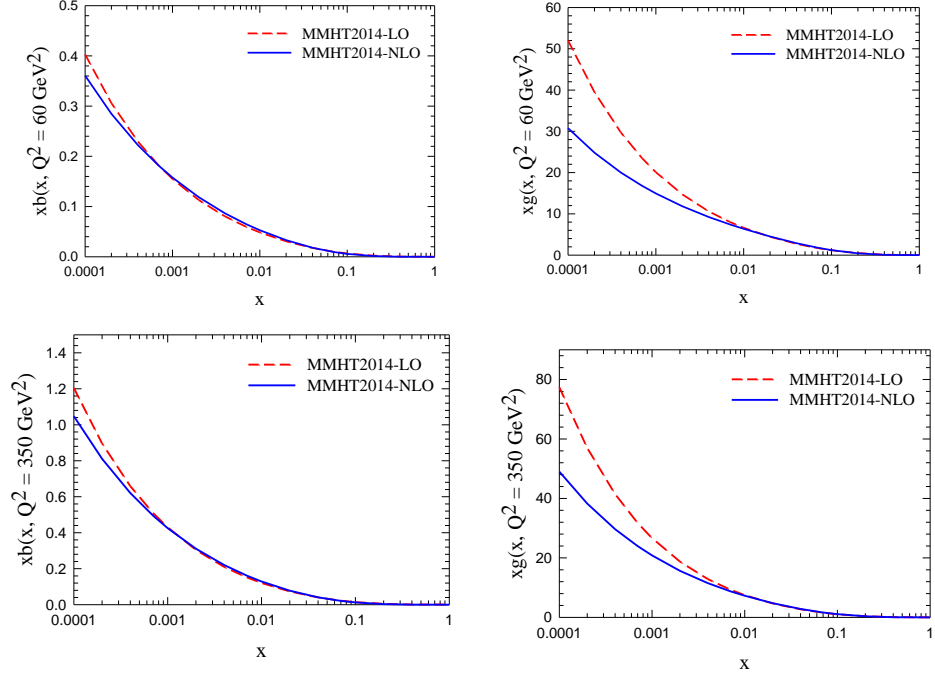


FIG. 4: The integrated beauty quark and gluon distribution functions at scale $Q^2 = 60$ and 350 GeV^2 , by using the *MMHT2014-LO* (dashed curves) and *MMHT2014-NLO* (full curves) [21].